

Materials Advances

Volume 1
Number 7
October 2020
Pages 2141–2546

rsc.li/materials-advances



ISSN 2633-5409

COMMUNICATION

Yasukazu Kobayashi *et al.*
Simple chemical synthesis of intermetallic Pt₂Y bulk
nanopowder

Simple chemical synthesis of intermetallic Pt₂Y bulk nanopowder†Yasukazu Kobayashi,^a Shohei Tada^b and Ryuji Kikuchi^cCite this: *Mater. Adv.*, 2020, 1, 2202Received 15th June 2020,
Accepted 3rd August 2020

DOI: 10.1039/d0ma00419g

rsc.li/materials-advances

Intermetallic Pt₂Y bulk nanopowder (2.9 m² g^{−1}, 28 nm) was chemically obtained from H₂PtCl₆·6H₂O and Y₂O₃ that were finally reduced and alloyed in molten LiCl–CaH₂ under Ar at 600 °C. It is a novel simple approach to obtain nanopowders with no gloveboxes, vacuum systems, or even organic solvents.

Platinum is the most widely used oxygen reduction reaction (ORR) catalyst in fuel cells due to its excellent catalytic performance.^{1,2} Since Pt is expensive and rare, alloying catalysts have been intensively studied in order to decrease the platinum amount required, and to improve the performances of activity and stability. Among them, Pt–Y alloy is one of the most attractive and promising candidates due to the improved performances confirmed by several research groups.^{3,4} However, it is a significantly challenging task to prepare alloy nanostructures for actual applications, mainly because yttrium has a very strong oxygen affinity to form Y₂O₃ readily and the oxide is hardly reducible.⁵ Therefore, most successful reports of Pt–Y nanoparticles have been made *via* a physical top-down approach, such as advanced sputtering techniques,^{6,7} in which the nanoparticles were commonly prepared from the pure metals under a highly clean environment of oxygen-/moisture-tight conditions.⁸

On the other hand, a more challenging chemical approach has recently been attempted ardently to obtain Pt–Y nanostructures because the approach has a more scalable potential. Kanady *et al.* successfully prepared intermetallic Pt₃Y nanoparticles of 5–20 nm by a molten salt reducing approach with molten borohydride (KEt₃BH) both as a strong reducing agent and a reaction medium.⁹ Roy *et al.* synthesized carbon-supported Pt_xY nanoparticles by a hydrogen-reduction of YCl₃ at 600–800 °C,

while keeping very low ppm-range concentrations of O₂ and H₂O in the system.¹⁰ Hu *et al.* reported intermetallic Pt₃Y nanoparticles prepared from the reduction of an oxygen-free yttrium carbodiimide precursor that is insensitive to O₂ and H₂O.¹¹ Reported chemical approaches are well summarized in a current reviewed paper in more detail.¹² Thus, the total reduction of yttrium species in a highly clean environment is a key strategy to obtain Pt–Y alloy nanostructures successfully.

In this study, we report a novel chemical approach to obtain intermetallic Pt₂Y bulk nanopowder *via* a simple molten salt reduction.^{13–16} In the method, Pt/Y₂O₃ precursor was totally reduced under argon flow in a physical mixture with LiCl and CaH₂ powders at 600 °C, at which temperature the mixed LiCl was in a molten salt form. Apart from the previous molten salt approach,⁹ LiCl and CaH₂ are commonly approachable powder chemicals at room temperature and allow for easy handling without any special facilities, such as glove boxes and vacuum systems. CaH₂ was additionally mixed as a reducing agent to extract oxygen from yttrium oxides in the reduction process. No organic solvents, dangerous chemicals, or explosive gases were used in the method. Even in critical comparison with previous chemical methods, our proposed approach in this study is the simplest method ever to prepare Pt–Y nanostructures, thus leading to a scalable application.

Intermetallic Pt₂Y bulk nanopowder was prepared by reducing a Pt/Y₂O₃ precursor in the molten LiCl–CaH₂ system. First, H₂PtCl₆·6H₂O (Wako Pure Chem. Corp.) was dissolved in distilled water, and after mixing the solution well, Y₂O₃ (Sigma-Aldrich Co. LLC) was suspended into the solution in a molar ratio of Pt/Y = 3/1. The platinum-rich ratio was required to obtain a Pt₂Y phase. While stirring the suspension, it was kept heating at 110 °C overnight. The dried powder was then preliminarily heated at 300 °C and finally at 500 °C in air for 2 h in order to obtain the Pt/Y₂O₃ precursor. Next, the precursor was mixed with CaH₂ (JUNSEI Chem. Co. Ltd) and LiCl (Wako Pure Chem. Corp.) in a mortar in a weight ratio of precursor/CaH₂/LiCl = 1/2/1. The mixed powder was then loaded into a stainless steel reactor and heated at 600 °C for 2 hours under an argon gas flow.

^a Interdisciplinary Research Center for Catalytic Chemistry, National Institute of Advanced Industrial Science and Technology (AIST), 1-1-1 Higashi, Tsukuba, Ibaraki 305-8565, Japan. E-mail: yasu-kobayashi@aist.go.jp

^b Department of Materials Science and Engineering, Ibaraki University, 4-12-1 Nakanarusawacho, Hitachi, Ibaraki 316-8511, Japan

^c Department of Chemical System Engineering, The University of Tokyo, 7-3-1 Hongo, Bunkyo-ku, Tokyo 113-8656, Japan

† Electronic supplementary information (ESI) available. See DOI: 10.1039/d0ma00419g

Finally, the reduced precursor was crushed in a mortar and rinsed with 0.1 M NH_4Cl aqueous solution to dissolve impure species, such as CaH_2 , CaO , and LiCl , and finally by distilled water in order to obtain the final reduced powder.

The crystal structure was analysed by X-ray diffraction (XRD, SmartLab (3 kW), Rigaku) with $\text{CuK}\alpha$ radiation at 40 kV and 45 mA. The porosity was examined by N_2 adsorption at -196°C (BELLSORP mini-II, Microtrac-BEL). Before the measurement, the sample powder was pretreated at 200°C for 30 min under a vacuum, and the contained water was removed. The morphology was observed by scanning electron microscopy (SEM, JSM-7800F, JEOL Ltd) and transmission electron microscopy (TEM, a Tecnai Osiris, FEI system) with energy dispersive X-ray spectrometry (EDS) for elemental analysis. Metallic/oxidation states of platinum and yttrium in the final sample were confirmed by X-ray photoelectron spectroscopy (XPS, PS-9010, JEOL Ltd). The spectra were corrected by referencing the binding energy to carbon (C 1s 284.6 eV). We used the XPSPEAK4.1 to analyse the obtained spectra. Commercial Pt/C (type STD, Wako Pure Chem. Corp.) and Y_2O_3 (Wako Pure Chem. Corp.) were used for comparison.

Fig. 1 shows the XRD patterns of the precursor and the final reduced powder. For the precursor, the observed peaks were totally identified to Pt metal. No clear peaks of Y_2O_3 were observed, but a very broad signal was slightly obtained over $30\text{--}40^\circ$ that could be assigned to amorphous yttrium oxide. For the reduced powder, the observed peaks were attributed mainly to an intermetallic Pt_2Y and partly to Pt metal at 46.2° . Since the precursor had a Pt/Y ratio of 3/1, the reduced powder could be composed of Pt_2Y and Pt phases. A peak corresponding to a (111) facet at 20.2° seemed higher than the reference one, probably indicating that the facet had grown preferentially in the intermetallic Pt_2Y phase.

Fig. 2 and Fig. S1 (ESI †) show SEM images of the reduced Pt_2Y powder. The appearance looks quite porous and the porous structure seems composed of very small nanoparticles

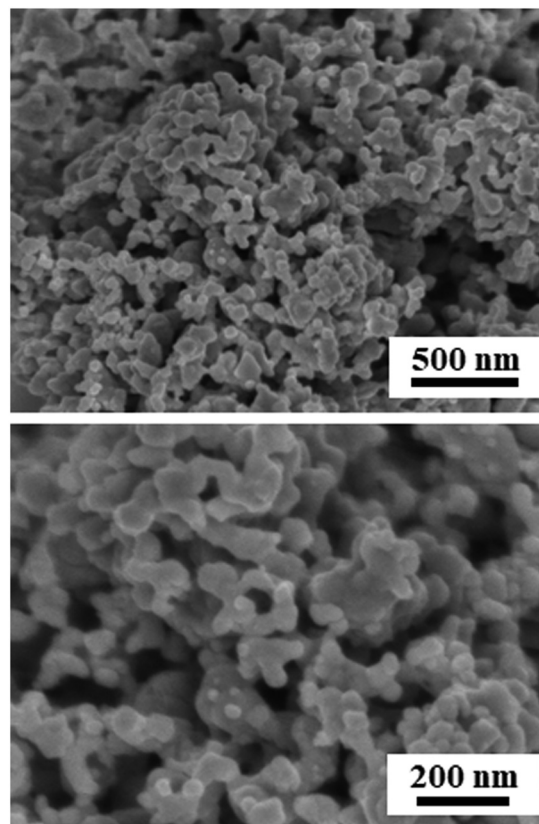


Fig. 2 SEM images of the reduced Pt_2Y bulk nanopowder.

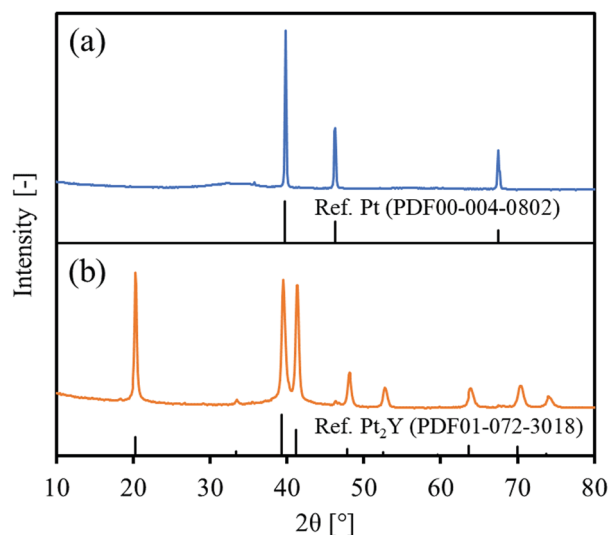


Fig. 1 XRD patterns of (a) a precursor and (b) the reduced Pt_2Y bulk nanopowder with references.

interconnected with one another. The particle size distribution is relatively broad, but nano-sized spheres of <100 nm are clearly seen from the images. The nano-sized morphology was also confirmed by TEM observations (Fig. S2, ESI †), and it was likely to be polycrystalline compounds, from the magnified images (Fig. S3, ESI †). According to the results of elemental analyses by SEM-EDS (Fig. S4 and S5, ESI †) and TEM-EDS (Fig. 3 and Fig. S6, ESI †), uniform distributions are seen for both Pt and Y and they correspond with each other well. The obtained Pt/Y molar ratios were 4.5/1.0 and 3.8/1.0, respectively. Some particles were also observed as indicated in Fig. S7 (ESI †), and they were platinum metals in most cases, according to the EDS analyses. Small amounts of calcium were detected by EDS analyses of both, but they were negligible enough, so it indicated that any calcium-related impurity species were appropriately washed out by the post-rinsing treatments by NH_4Cl aqueous solution.

Fig. 4 shows the XPS spectra of the reduced Pt_2Y bulk nanopowder. The detailed information on the deconvoluted peaks is summarized in Tables S1 and S2 (ESI †). In comparison with the Y_2O_3 reference, Pt_2Y shows a broad spectrum corresponding to yttrium 3d. The spectrum observed over a high binding energy region that is nearly overlapped with Y_2O_3 was identified to be $3d_{5/2}$ and $3d_{3/2}$ of Y_2O_3 , whereas that corresponding to separated peaks at 155 eV and 157 eV could be $3d_{5/2}$ and $3d_{3/2}$ peaks of metallic yttrium, respectively.⁹ Thus, it was suggested that the Pt_2Y surface was composed of metallic yttrium and yttrium oxide. The existence of oxides was also



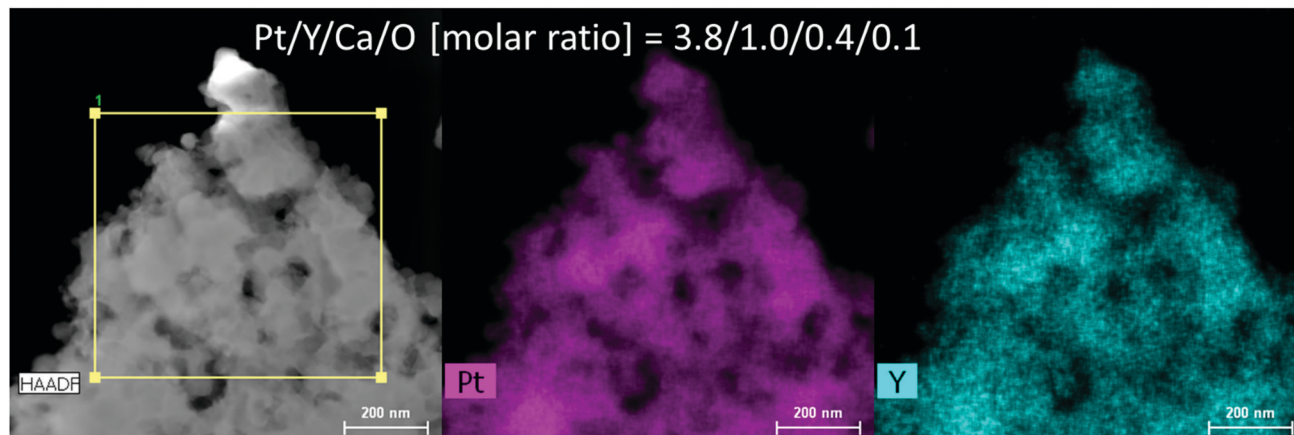


Fig. 3 Results of TEM-EDS for the reduced Pt_2Y bulk nanopowder. The EDS spectrum is depicted as Fig. S6 (ESI[†]).

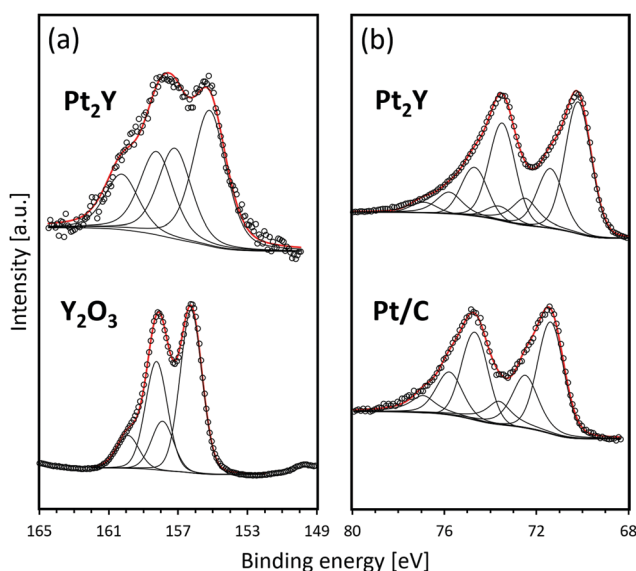


Fig. 4 XPS spectra of (a) Y 3d and (b) Pt 4f for the reduced Pt_2Y bulk nanopowder and the references of Y_2O_3 and Pt/C, respectively. Open circles are experimental data, and red lines are the fitting curves separated into some peaks.

indicated by EDS analyses (Fig. S4 and S5, ESI[†]). The surface layer of yttrium oxide is considered to be a cumbersome issue in view of the actual catalysis application. Still, the easy removal has been confirmed by acid treatments afterward to activate the surface for superior catalytic performances.^{9,11} As for platinum 4f, a similar spectrum to a reference Pt/C was observed. Of note, two extra peaks appear in a lower binding energy region (70.2 eV for $4f_{7/2}$ and 73.5 eV for $4f_{5/2}$). The shift indicates the electron donation from yttrium to platinum throughout the metallic bonds as reported.^{4,5}

The average particle size of interconnected nanoparticles observed in the SEM and TEM images of the reduced Pt_2Y powder was estimated from the nitrogen adsorption experiment (Fig. S8, ESI[†]) and XRD measurement. As given in Table 1, the measured BET surface area was $2.9 \text{ m}^2 \text{ g}^{-1}$, and the estimated particle size from the surface area was 147.8 nm. Because the approximate particle size is less than a few hundred nanometers

Table 1 BET surface area (SA) and particle size of reduced Pt_2Y nanoparticles obtained by nitrogen adsorption and XRD measurement

BET SA [$\text{m}^2 \text{ g}^{-1}$]	Particle size [nm]	
	N_2 ads. ^a	XRD ^b
2.9	147.8	28.2

^a Assumed that the sample was composed of non-porous spherical Pt_2Y with the density of 13.90 g cm^{-3} . ^b Calculated by the Scherrer equation with a main peak at 20.3° .

as visible from the SEM and TEM images, the estimated size is considered reasonable and proper. In addition, the particle size is much larger than the crystallite size obtained by the Scherrer equation (28.2 nm), and this difference suggests that the Pt_2Y nanoparticles prepared in this study could be polycrystalline.

Conclusions

Intermetallic Pt_2Y bulk nanopowder with a defined crystal structure and a nano-sized morphology was obtained *via* a simple chemical approach. No special facilities and chemicals were required to obtain the nanopowder but common chemicals, such as LiCl and CaH_2 .

A part of this work was conducted at Advanced Characterization Nanotechnology Platform of the University of Tokyo, supported by “Nanotechnology Platform” of the Ministry of Education, Culture, Sports, Science and Technology (MEXT), Japan. We acknowledge Center for Instrumental Analysis, Ibaraki University for the XPS measurements.

Conflicts of interest

There are no conflicts to declare.

References

- C. Kim, F. Dionigi, V. Beermann, X. Wang, T. Möller and P. Strasser, *Adv. Mater.*, 2019, **31**, 1805617.
- M. Liu, Z. Zhao, X. Duan and Y. Huang, *Adv. Mater.*, 2019, **31**, 1802234.



- 3 J. Greeley, I. E. L. Stephens, A. S. Bondarenko, T. P. Johansson, H. A. Hansen, T. F. Jaramillo, J. Rossmeisl, I. Chorkendorff and J. K. Nørskov, *Nat. Chem.*, 2009, **1**, 552.
- 4 S. J. Hwang, S.-K. Kim, J.-G. Lee, S.-C. Lee, J. H. Jang, P. Kim, T.-H. Lim, Y.-E. Sung and S. J. Yoo, *J. Am. Chem. Soc.*, 2012, **134**, 19508.
- 5 T. Ogawa, Y. Kobayashi, H. Mizoguchi, M. Kitano, H. Abe, T. Tada, Y. Toda, Y. Niwa and H. Hosono, *J. Phys. Chem. C*, 2018, **122**(19), 10468.
- 6 P. Hernandez-Fernandez, F. Masini, D. N. McCarthy, C. E. Strebel, D. Friebe, D. Deiana, P. Malacrida, A. Nierhoff, A. Bodin, A. M. Wise, J. H. Nielsen, T. W. Hansen, A. Nilsson, I. E. L. Stephens and I. B. Chorkendorff, *Nat. Chem.*, 2014, **6**, 732.
- 7 R. Brown, M. Vorokhta, I. Khalakhan, M. Dopita, T. Vonderach, T. Skála, N. Lindahl, I. Matolínova, H. Gronbeck, K. M. Neyman, V. Matolin and B. Wickman, *ACS Appl. Mater. Interfaces*, 2020, **12**, 4454.
- 8 Y. Lu, J. Li, T.-N. Ye, Y. Kobayashi, M. Sasase, M. Kitano and H. Hosono, *ACS Catal.*, 2018, **8**(12), 11054.
- 9 J. S. Kanady, P. Leidinger, A. Haas, S. Titlbach, S. Schunk, K. Schierle-Arndt, E. J. Crumlin, C. H. Wu and A. P. Alivisatos, *J. Am. Chem. Soc.*, 2017, **139**, 5672.
- 10 C. Roy, B. P. Knudsen, C. M. Pedersen, A. Velázquez-Palenzuela, L. H. Christensen, C. D. Damsgaard, I. E. L. Stephens and I. B. Chorkendorff, *ACS Catal.*, 2018, **8**, 2071.
- 11 Y. Hu, J. O. Jensen, L. N. Cleemann, B. A. Brandes and Q. Li, *J. Am. Chem. Soc.*, 2020, **142**, 953.
- 12 S. G. Peera, T. G. Lee and A. K. Sahu, *Sustainable Energy Fuels*, 2019, **3**, 1866.
- 13 Y. Kobayashi, *Chem. Lett.*, 2019, **48**, 1496.
- 14 Y. Kobayashi, S. Tada and R. Kikuchi, *Chem. Lett.*, 2020, **49**, 341.
- 15 Y. Kobayashi, S. Tada and R. Kikuchi, *Mater. Trans.*, 2020, **61**, 1037.
- 16 Y. Kobayashi, S. Tada and R. Kikuchi, *J. Chem. Eng. Jpn.*, in press.

